TRANSPORTATION SCIENCE
Vol. 40, No. 3, August 2006, pp. 351–363
ISSN 0041-1655 | EISSN 1526-5447 | 06 | 4003 | 0351

DOI 10.1287/trsc.1050.0137
© 2006 INFORMS

Performance and Design of Mobility Allowance Shuttle Transit Services: Bounds on the Maximum Longitudinal Velocity

Luca Quadrifoglio, Randolph W. Hall, Maged M. Dessouky
Daniel J. Epstein Department of Industrial and Systems Engineering, University of Southern California, Los Angeles, California 90089-0193 {quadrifo@usc.edu, rwhall@usc.edu, maged@usc.edu}

We develop bounds on the maximum longitudinal velocity to evaluate the performance and help the design of mobility allowance shuttle transit (MAST) services. MAST is a new concept in transportation that merges the flexibility of demand responsive transit (DRT) systems with the low-cost operability of fixed-route bus systems. A MAST system allows buses to deviate from the fixed path so that customers within the service area may be picked up or dropped off at their desired locations. However, the main purpose of these services should still be to transport customers along a primary direction. The velocity along this direction should remain above a minimum threshold value to maintain the service attractive to customers. We use continuous approximations to compute lower and upper bounds. The resulting narrow gap between them under realistic operating conditions allows us to evaluate the service in terms of velocity and capacity versus demand. The results show that a two-vehicle system, with selected widths of the service area of 0.5 miles and 1 mile, is able to serve, respectively, a demand of at least 10 and 7 customers per longitudinal mile of the service area while maintaining a reasonable forward progression velocity of about 10 miles/hour. The relationships obtained can be helpful in the design of MAST systems to set the main parameters of the service, such as slack time and headway.

Key words: public transportation; transit service design; performance; continuous approximations
History: Received: October 2004; revision received: July 2005; accepted: October 2005.

DO NOT Distribute or Reproduce
Author's Personal Copy

1. Introduction

Traditional fixed-route bus transit systems are cost efficient for a wide range of operations owing to the loading capacity of the buses as well as trip and passenger consolidations (e.g., ridesharing). However, the general public considers the service to be inconvenient because either the locations of the pick-up and drop-off points do not, or the schedule of the service does not, match the individual rider's desires (lack of flexibility). Flexible systems such as demand responsive transit (DRT) networks tend to be much more costly to deploy as a general transit service than fixed-route bus systems. Hence, DRT systems are largely limited to specialized operations such as dial-a-ride (mandated under the Americans with Disabilities Act), taxicab, or shuttle van services.

Thus, there is a need for a transit system that provides flexible service at a cost-efficient price. The mobility allowance shuttle transit (MAST) system is one such concept that merges the flexibility of DRT systems with the low-cost operability of fixed-route bus systems. A MAST service has a fixed-base route that covers a specific geographic zone, with a set of mandatory checkpoints with fixed scheduled departure times conveniently located at major connection points or at high-density demand zones; the innovative twist is that, given an appropriate slack time, buses are allowed to deviate from the fixed path to pick up and drop off passengers at their desired locations. The only restriction on flexibility is that the deviations must lie within a predetermined distance from the fixed-base route. Customers can be of three types: *hybrid* (having one service point at noncheckpoint location in the service area and the other one at the checkpoints), *regular* (both service points at the checkpoints), or *random* (both service points located at noncheckpoint stops). Customers make a reservation to add their desired pick-up and/or drop-off stops in the schedule of the service. Regular customers do not need a booking process to use the service.

Such a system already exists in a reduced and simplified scale. The Metropolitan Transit Authority (MTA) of Los Angeles County, California, introduced MAST as part of its feeder Line 646. During the day, this line operates as a regular fixed-route bus system. At night, the line changes to a MAST service with three checkpoints and a total service area of 12×0.5 miles^2 (6 miles of length between each pair of checkpoints). Customers may call in to be picked up, or may ask the operator to be dropped off at their desired locations if within the service area. Most of the customers (80%) are hybrid, and the remaining

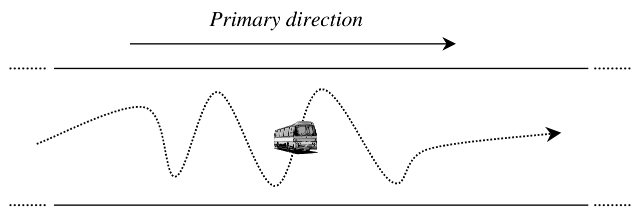

Figure 1 **Primary Direction of MAST Services**

20% is evenly distributed among regular and random types.

In the case of public transport, the main purpose of these systems is to move customers along a primary direction (see Figure 1), which may be around a loop or back and forth between two terminal checkpoints. A higher demand served per vehicle would allow the service to be more cost efficient. However, the more demand that is served, the slower the vehicles would move because of the deviations and service time needed for pick-ups and drop-offs, causing the service to become less attractive to customers.

The purpose of this paper is to model the relationship between the velocity along the primary direction of a MAST service and the demand to assess the performance of these types of systems and help in the design process. A minimum threshold value of the velocity can be used to set the maximum slack time allowable between checkpoints and to determine the maximum demand level that can be served by one vehicle and the number of vehicles to be employed per line to serve all demand.

The computation of the velocity of the vehicle along the primary direction depends on solving the vehicle routing problem among the demand points, which is a known NP-hard problem. Even though some real problems are small enough to solve optimally by enumeration, we utilize continuous approximation assumptions to provide upper and lower bounds of the maximum velocity of the vehicle between pairs of consecutive checkpoints at different demand levels. This analytical effort develops relationships for higher demand as well creates methodology to quickly evaluate different design scenarios. We then plot the relationship between the velocity and the demand to evaluate the performance of the system at different demand levels and provide insights on the design of the system.

The remainder of this paper is divided as follows. Section 2 provides a literature review. Section 3 defines the system. Section 4 provides the lower bound of the optimal longitudinal velocity. Section 5 discusses the optimality of the no-backtracking routing policy needed to obtain the first upper bound presented in §6. Section 7 derives the second upper bound. Sections 8 provide an estimate of the velocity from an approximate formula. Section 9 discusses the performance and the design of the MAST service. Finally, §10 presents the conclusions.

2. Literature Review

MAST systems have been recently studied by researchers. Quadrifoglio, Dessouky, and Palmer (2006) developed an insertion algorithm to schedule a MAST system; in this paper the efficient use of control parameters significantly improved the performance of the algorithm. Zhao and Dessouky (2004) studied the optimal service capacity through a stochastic approach. Malucelli, Nonato, and Pallottino (1999) also approached the problem, including it in a general overview of flexible transportation systems. Crainic, Malucelli, and Nonato (2001) described the MAST concept and incorporated it in a more general network setting also providing a mathematical formulation. Other works studying a combination of fixed and flexible services can be found in Cortés and Jayakrishnan (2002), Horn (2002a, b), and Aldaihani and Dessouky (2003), which primarily focus on the operational control and scheduling of such systems. In this paper we utilize continuous approximations to estimate the values of the parameters of the system during the design phase. As noted by Daganzo (1991), the main purpose of this approach is to obtain reasonable solutions with as little information as possible. Hall (1986) also pointed out that continuous approximations are useful in developing models that are easy to comprehend; on the other hand, he observed that these models should not replace but supplement the more detailed mathematical programming models.

There is a significant body of work in the literature on continuous approximation models for transportation systems. Most of the work has been developed to provide decision-support tools for strategic planning in the design process. Langevin, Mbaraga, and Campbell (1996) provide a detailed overview of the research performed in the field. They concentrate primarily on freight distribution systems while in this paper we focus on public transport, but most of the issues of interest are common to both fields.

Pioneering research on continuous approximation models dates back to the 1950s Beardwood, Halton, and Hammersley (1959) provided the first approximation formula to estimate the length of a traveling salesman problem (TSP) tour in a compact zone with uniform demand density. Stein (1978) and Jaillet (1988) integrated their work by estimating the value of the TSP tour length in case of Euclidean and rectilinear metrics. In general, geometrical probability has been extensively studied to provide estimates on the average distances among points for different shapes. We mention in this area the work of Ghosh (1951), Fairthorne (1965), Schweitzer (1968),

Author's Personal Copy
DO NOT Distribute or Reproduce

Christofides and Eilon (1969), Bouwkamp (1977), Ruben (1978), Daganzo (1980, 1984b), Vaughan (1984), Koshizuka and Kurita (1991), and Stone (1991). Similar works on estimating TSP length have been developed from a more theoretical and multidimensional point of view by Verblunsky (1951), Rhee (1993), and Stadje (1995). The work of Daganzo (1984a) is especially related to this paper because it introduces the concept of "strip strategy," providing an approximate estimate of the optimal width of a corridor to minimize the distance between points and therefore the length of the TSP tour, while employing a simple no-backtracking routing policy along the strip. In our paper, the MAST system's service area has been modeled as a corridor.

Szplett (1984) provides a review of the research performed on continuous models specifically for public transport. In this area we cite the work of Newell (1979), Mandl (1980), Ceder and Wilson (1986), LeBlanc (1988), Chang and Schonfeld (1991a, b), Chien and Schonfeld (1997), and Aldaihani et al. (2004) that studied the optimality of bus network systems. Lesley (1976a, b), Wirasinghe and Ghoneim (1981), and Kuah and Perl (1988) analyzed the optimality of spacing between bus stops.

Continuous models have also been utilized to examine DRT systems. Daganzo (1978) used an approximate analytical model to study many-to-many DRT systems; Daganzo (1984c) also analytically studied a transportation system, where centralized checkpoints are used to cluster together the random demand. Jacobson (1980) made use of an analytical model for DRT systems as well. Diana, Dessouky, and Xia (2006) provide an analytical model to determine the fleet size of a DRT system.

3. System Definition

The model considered for our analysis consists of a rectangle of width w and length $L > w$ oriented in a horizontal direction, representing a segment of a MAST system delimited by two consecutive checkpoints with coordinates $(0, w/2)$ and $(L, w/2)$. The complete MAST system would have similar segments adjacent to the one considered, on the right or left. The demand is assumed to be known in advance and is represented by a set of stops (either pick-ups or drop-offs) uniformly distributed across the width and the length of the rectangle, with density 2ρ per unit area. If the number of regular and random customers are the same (as for the real MAST Line 646 in Los Angeles), the density of the customers is also 2ρ. For purpose of illustration, we assume that vehicles travel with constant speed v, have infinite loading capacity, and follow rectilinear paths within the rectangle. Dessouky, Ordóñez, and Quadrifoglio (2005) show that these two latter assumptions are quite reasonable. At the pick-up/drop-off points, there is a constant service time of s.

Vehicles follow a forward progression through the rectangle in either a left-right or right-left direction. This means that a left-right (right-left) vehicle travels from the left (right) checkpoint to the right (left) checkpoint of the rectangle and only serves pick-up stops whose corresponding drop-off is to their right (left) or drop-off stops whose corresponding pick-up is to their left (right). This is only a reasonable operating policy, but not necessarily optimal. Note that the corresponding pick-up (drop-off) of each stop could be within or outside the segment considered or at one of the checkpoints (see Figure 2).

The general system is represented by several vehicles traveling along the rectangle, but we assume that 2ρ represents one cycle of the demand served by two vehicles: a left-right one and a right-left one. The problem is symmetrical and we analyze only the left-right case, with a demand density per unit area of ρ stops.

The total number of left-right (or right-left) stops in the rectangle is given by

$$n = \rho w L. \tag{1}$$

The longitudinal velocity V of the vehicle is defined by the rate at which the vehicle moves in the horizontal direction that has the average given by

$$V = \frac{L}{t} = \frac{L}{p/v + ns} \tag{2}$$

where t is the total time spent by the vehicle while traveling between two checkpoints, p is the length of a rectilinear Hamiltonian path among all the service points (respecting the customer precedence constraints), and ns represents the total service time (ignoring the checkpoints).

We assume that the problem (P) is simply to minimize p (with optimal value p^*), which corresponds to maximize V (with optimal value V^*), to evaluate the maximum possible demand served by the system for each V. We do not consider other performance measures such as total waiting time and total passenger time, essential for more accurate analyses

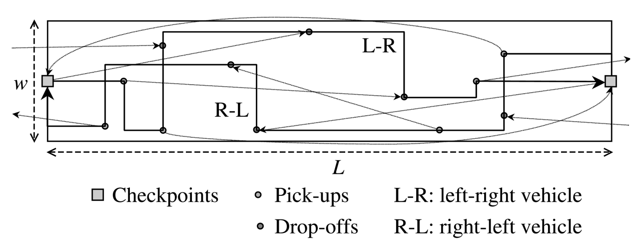

Figure 2 Right-Left and Left-Right Vehicles

Author's Personal Copy
DO NOT Distribute or Reproduce

at the operational level (Quadrifoglio, Dessouky, and Palmer 2006).

The system parameters and the notation used in the paper are as follows.

- w width of rectangle (miles)
- L length of the rectangle (miles); $L > w$
- v average vehicle speed (miles/hour)
- s service time for pick-up/drop-off (hours)
- ρ demand density of the "left-right" stops (stops/miles^2)
- V longitudinal velocity of the vehicle (miles/hour)
- V^* optimal (maximum) value of V
- $i = 1, \ldots, n \in \mathrm{N}$ set of all "left-right" stops (pick-ups and drop-offs)
- x_i longitudinal coordinate of i, increasing from left to right (miles)
- y_i lateral coordinate of i, increasing from bottom to top (miles)

We use $v = 30$ miles/hour and $s = 30$ seconds in all the experiments performed throughout the paper.

4. Lower Bound of V

Let us consider a no-backtracking policy, allowing the vehicle to move only in the forward direction (left to right) and serve all the demand, as illustrated in Figure 3. Because by assumption the customers served by a left-right vehicle have their drop-off always on the right of their pick-up, this policy guarantees feasibility because all origins are served before their destination points, satisfying all customer precedence constraints. However, this policy is not necessarily optimal. In fact, the solution could be improved by simply removing the arbitrary no-backtracking constraint and developing a better routing strategy. Thus, this simple no-backtracking policy provides a feasible lower bound on the expectation of V^*, but it does not provide optimality. For our purpose the policy is useful because we can compute a closed-form expression for a bound velocity.

The longitudinal velocity is given by Equation (2), where the rectilinear Hamiltonian path p is the sum of the distance traveled longitudinally by the vehicle (that is simply L, because we are assuming a no-backtracking policy) plus the distance traveled laterally (along the vertical direction). Let l_y be a random variable indicating the lateral distance traveled

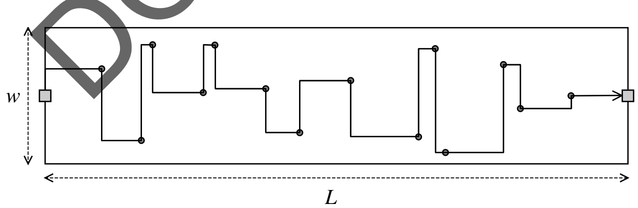

Figure 3 No-Backtracking Policy

between any pair of stops in the rectangle and l'_y be a random variable indicating the lateral distance traveled from/to a checkpoint to/from any stop in the rectangle. Laterally, the vehicle will travel l'_y from the starting checkpoint to the first stop, then l_y for $n-1$ times between each pair of stops and l'_y from the last stop to the ending checkpoint. With uniform demand the expected values of l_y and l'_y are given by

$$E[l_y] = \frac{w}{3} \quad \text{and} \tag{3}$$

$$E[l'_y] = \frac{w}{4}. \tag{4}$$

Therefore, for a no-backtracking policy the expected values of p and t in Equation (2) are given by

$$E[p] = L + 2E[l'_y] + (n-1)E[l_y] = \frac{\rho w^2 L}{3} + L + \frac{w}{6} \quad \text{and} \tag{5}$$

$$E[t] = \frac{E[p]}{v} + ns = \rho w L\left(\frac{w}{3v} + s\right) + \frac{L}{v} + \frac{w}{6v}. \tag{6}$$

The expected value of the lower bound on V^* is $E[L/t]$, which is very well approximated and lower bounded by $L/E[t]$ (from the Jensen inequality: For a random variable z, $E[1/z] \geq 1/E[z]$). Therefore, we compute the lower bound V^L by

$$E\left[\frac{L}{t}\right] \geq V^L = \frac{L}{E[t]} = \frac{v}{1 + \rho w(sv + w/3) + w/(6L)}. \tag{7}$$

Note that V^L is inversely proportional to w, s, and ρ.

We can verify that Jensen's inequality produces a tight bound in the following Table 1, which shows that Equation (7) provides a good estimate of the true lower bound $E[L/t]$ computed by simulation for different values of ρ. The simulation values are obtained by averaging 10,000 replications for each ρ considered. In each replication we considered a corridor with $w = 0.5$ miles and $L = 6$ miles.

5. Optimality of No-Backtracking Policy

Before estimating the first upper bound we want to focus on the *strip strategy* introduced by Daganzo

Table 1 V^L **Values: Analytical vs. Simulation**

	V^L (miles/hour)	
ρ	Equation (7)	Simulation
1	24.54	24.56
5	14.59	14.61
10	9.69	9.70
50	2.62	2.63
100	1.37	1.37

Author's Personal Copy
DO NOT Distribute or Reproduce

(1984a). He showed that good solutions of the TSP tour, for any shape of the service area, are obtained by cutting a swath covering the whole area and having the vehicle drive along the resulting long strip while serving the demand uniformly distributed in the area. He claimed that by selecting a proper width of the strip a simple no-backtracking policy produces good results in terms of the total distance traveled.

We want to determine if there exists any sufficient condition on the locations of the demand points that would guarantee optimality of a no-backtracking routing policy. This would allow us to select a subset of points that satisfy this condition so that we can utilize the no-backtracking routing policy to serve them optimally. The longitudinal velocity to serve this subset will be an upper bound on V^*.

To find out whether this sufficient condition exists, let us consider a left-right vehicle following a Hamiltonian path (α) among a set of demand points. Referring to Figure 4, consider points j, h, and k. We assume that $x_h \leq x_j$ and $x_h \leq x_k$ and that the backtracking subsequence $\ldots$–j–h–k–$\ldots$ is part of path α. We want to determine if there exists a condition on x_h with respect to x_j and x_k to guarantee that a reinsertion of h earlier in the schedule in a no-backtracking fashion will always lead to a shorter total distance traveled.

We note that it is always possible to identify two consecutive points a and b earlier in the schedule such that $x_a \leq x_h \leq x_b$ (at the limit, we can have a be the starting checkpoint on the left and/or $b \equiv j$). Therefore, we have path α following the sequence $\ldots$–a–b–$\ldots$–j–h–k–$\ldots$.

Consider another path (β) that follows the sequence …–a–h–b–…–j–k–… with point h reinserted between a and b in a no-backtracking fashion.

Let us compute the rectilinear distance driven in the two cases, considering only the relevant portions of the sequences that differ between α and β. Path α yields to the following distance l_α:

$$l_\alpha = x_b - x_a + |y_b - y_a| + x_j - x_h + |y_j - y_h| + x_k - x_h + |y_k - y_h|. \tag{8}$$

For the path β the distance l_β is given by

$$l_\beta = x_h - x_a + |y_h - y_a| + x_b - x_h + |y_b - y_h| + |x_k - x_j| + |y_k - y_j|. \tag{9}$$

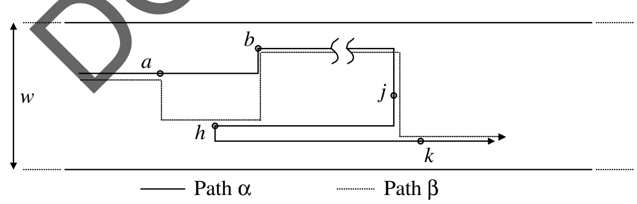

Figure 4 **Two Different Paths to Serve Points** a, b, j, h, k

We want to determine the minimum longitudinal distance between h and j and/or h and k needed to guarantee that path β will always be better than path α in terms of minimizing the total distance traveled. Therefore, we impose the condition $l_\beta \leq l_\alpha$ and after a few passages we obtain the following inequality:

$$\begin{aligned} x_j + x_k - |x_k - x_j| - 2x_h &\geq |y_h - y_a| + |y_b - y_h| - |y_b - y_a| \\ &\quad + |y_k - y_j| - |y_j - y_h| - |y_k - y_h|. \end{aligned} \tag{10}$$

Depending on the random vertical position of the points along the corridor, the maximum possible value for $|y_h - y_a| + |y_b - y_h| - |y_b - y_a|$ is $2w$ when h is located on the opposite edge of the corridor with respect to a and b, while $|y_k - y_j| - |y_j - y_h| - |y_k - y_h|$ can be at most equal to 0 when h is located laterally in between j and k. Otherwise, it is less than 0. Therefore, the right-hand side of Equation (10) is less than or at most equal to $2w$ and we have that the inequality becomes

$$\min(x_j, x_k) - x_h \geq w. \tag{11}$$

This is the sufficient condition on the longitudinal position of h, with respect to the closest (longitudinally) point between j and k, that would guarantee that the reinsertion of h somewhere earlier in the schedule in a no-backtracking fashion between some points a and b would always lead to a better solution in terms of shorter distance traveled.

Given the result obtained by Equation (11) we can state the following:

Proposition 1. *Given a set of points randomly distributed along a corridor of width w and length L, the shortest Hamiltonian rectilinear path from the first point on the far left to the last point on the far right is the sequence of points ordered by increasing longitudinal coordinate (no backtracking), as long as the minimum longitudinal distance between any pair of points is at least w.*

Proof. Consider a set of points identified by $i = 1, 2, 3, \ldots \in \mathrm{I}$ and ordered by increasing longitudinal coordinate (no backtracking), and let the minimum longitudinal distance between any pair of points be at least w. Assume that there exists an optimal sequence Λ ordered not following a no-backtracking policy; the position of each i in Λ is identified by $\lambda(i)$. Let us consider the point with the smallest $i_0 \in \mathrm{I}$ s.t. $i_0 \neq \lambda(i_0) \in \Lambda$. We can show by Equation (11) that reinserting i_0 in Λ such that $i_0 = \lambda(i_0)$ and readjusting all other $\lambda(i)$ accordingly leads to a better solution. However, this is a contradiction because we supposed Λ to be optimal. Therefore, the no-backtracking policy is optimal. □

DO NOT Distribute or Reproduce
Author's Personal Copy

6. First Upper Bound on V^*

To create an upper bound on V^* we first identify a subset $G[g(1), g(2), g(3), \ldots] \subseteq \mathrm{N}$ of points such that the longitudinal distance between any pair of them is as small as possible but at least w. By Proposition 1 we know that the optimal routing policy to serve the subset G is given by a no-backtracking sequence. We then assume that all the points $i \in \mathrm{N}$, but $i \notin G$, will be served as well but that no additional lateral deviations are required to reach them. This is a subproblem P′ (with optimal value p'^*) of the original problem P. We know by construction that $p'^* \leq p^*$, because in computing the total distance traveled in P′ we are ignoring some of the vertical deviations and possible backtracking portions of the path needed to attain p^*. Therefore, this policy guarantees optimality of the subproblem P′, without assuring feasibility of P, and represents a lower bound on the total minimum distance traveled (thus, an upper bound V^*).

To construct the subset G from the set N, we can use the following algorithm.

Algorithm 1.

1. $g(1)$ is the first point on the far left of the corridor.

2. $g(i+1)$ is the longitudinally closest point to the right of $g(i)$ after a "jump" of w units of length to the right of $g(i)$; with $i = 1, 2, 3, \ldots$.

3. Repeat Step 2 until there are no more points.

As an example, referring to Figure 5, we first include Point 1 in the subset G; then, from its horizontal coordinate x_1 we move w units of length to its right and we include in G the longitudinally closest point to the right of the location $x_1 + w$ (Point 6); and we proceed in this fashion including in G Points 9 and 14.

Let n_G be a discrete random variable representing the number of points in the subset G. If $n = 1$, $n_G = 1$. In the appendix, we compute analytically its expected value for $n = 2$ and $n = 3$, respectively given by Equations (33) and (37). With $w = 0.5$ miles and $L = 6$ miles we have $E[n_G \mid n = 2] \cong 1.84$ and $E[n_G \mid n = 3] \cong 2.56$ (verified by simulation). However, the distribution of n_G for higher values of n is not trivial to develop; thus, we estimate its expected value by the following continuous approximations.

The longitudinal positions at which points lie form (locally) a Poisson process with rate ρw. Thus, the expected value of the longitudinal distance l_x between two consecutive points in N is given by

$$E[l_x] = \frac{1}{\rho w}. \tag{12}$$

Whereas the longitudinal distance l'_x between two consecutive points in G forms a renewal process and its expected value is given by

$$E[l'_x] = w + E[l_x] = w + \frac{1}{\rho w} \tag{13}$$

where w is the minimum required distance between points in G.

The position of the first point in G is the longitudinally closest point on the right of the starting checkpoint, with an expected longitudinal coordinate of $E[l_x] = 1/\rho w$. With L/w large enough we can apply the central limit theorem and assume that $n_G - 1$ is normally distributed with mean $(L - E[l_x])/E[l'_x]$. Hence, the expected value of n_G can be estimated by

$$E[n_G] \cong 1 + \frac{L - E[l_x]}{E[l'_x]} = 1 + \frac{L - 1/(\rho w)}{w + 1/(\rho w)} = 1 + \frac{\rho w L - 1}{\rho w^2 + 1}. \tag{14}$$

The expected value of p is similar to Equation (4), with $E[n_G]$ replacing n. Thus, in this case the expected values of p and t are given by

$$E[p] = L + 2E[l'_y] + (E[n_G] - 1)E[l_y] = L + w\left[\frac{1}{2} + \frac{\rho w L - 1}{3(\rho w^2 + 1)}\right] \quad \text{and} \tag{15}$$

$$E[t] = \frac{E[p]}{v} + ns = \frac{L}{v} + \frac{w}{v}\left[\frac{1}{2} + \frac{\rho w L - 1}{3(\rho w^2 + 1)}\right] + \rho w L s. \tag{16}$$

Finally, the upper bound on V^* is formally given by $E[L/t]$, which is well approximated by $L/E[t]$ if t is sufficiently large (as it is, because its minimum possible value is $L/v + \rho w L s$) and $\mathrm{Var}[t]$ is low enough. Therefore, V^U is given by

$$V^U \cong \frac{L}{E[t]} = \frac{v}{1 + \rho w s v + \dfrac{w}{L}\left(\dfrac{1}{2} + \dfrac{\rho w L - 1}{3(\rho w^2 + 1)}\right)}. \tag{17}$$

As for V^L, V^U is inversely proportional to w, s, and ρ.

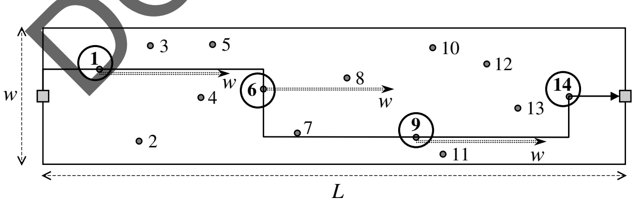

Figure 5 Subset G: Longitudinal Distance of at Least w Among Points

Authors Personal Copy
DO NOT Distribute or Reproduce

Table 2 V^U **Values: Analytical vs. Simulation**

	V^U (miles/hour)	
ρ	Equation (17)	Simulation
1	24.79	24.00
5	16.31	16.04
10	11.90	11.77
50	3.95	3.93
100	2.16	2.16

As done for V^L, we can demonstrate the accuracy of Equation (17) as a true upper bound for $E[L/t]$ through a set of examples computed by simulation for different values of ρ (10,000 replications for each ρ, with $w = 0.5$ miles, $L = 6$ miles), as shown in Table 2. Note that the simulation values are upper bounded by the values obtained with Equation (17).

7. Second Upper Bound on V^*

To produce the second upper bound we again remove constraints from problem P. The Hamiltonian path among all the points requires exactly one incoming arc and one outgoing arc at each node of the network so that all the points are connected to complete the tour. We remove the first assumption allowing unlimited incoming arcs at any node, but we still require exactly one outgoing arc from each node. In addition, we remove the customer precedence constraints. This is another subproblem P″ (with optimal value p''^*) of the original problem P. p''^* is given by the summation over all the stops of the arcs connecting any stop to its closest neighbor. In other words, we are stating that from each stop the vehicle has to travel at least to its closest neighbor; the sum over all stops produces p''^*, which is a lower bound on p^* and which therefore yields to an upper bound on V^*.

We know that uniformly and randomly scattered points follow (locally) a spatial Poisson distribution. Specifically, the number of points $\Gamma(A)$ within the area A is a Poisson random variable and its distribution is given by

$$P\{\Gamma(A) = q\} = \frac{(\rho A)^q}{q!} e^{-\rho A} \quad q = 0, 1, 2, 3, \ldots \tag{18}$$

with expected value equal to ρA.

Let D be the random variable indicating the distance of the closest neighbor from any stop $i \in \mathrm{N}$. We want to calculate $E[D]$. We can say that

$$F(d) = P\{D > d\} = P\{\Gamma[A(d)] = 0\} = e^{-\rho A(d)} \tag{19}$$

where $A(d)$ is the area around i within rectilinear distance d falling in the corridor. Depending on x, y, and d we can have nine different scenarios for the computation of $A(d)$, as shown in Figure 6. In the analysis we consider only the points $i \in \mathrm{N}$ located in a quarter of the rectangle ($0 \le x \le L/2$ and $0 \le y \le w/2$) because of its symmetry. We also ignore the effect of the right edge of the rectangle (at $x = L$).

Case 1. $A(d) = 2d^2$.

Case 2. $A(d) = 2d^2 - (d-y)^2 = d^2 + 2dy - y^2$.

Case 3. $A(d) = 2d^2 - (d-x)^2 = d^2 + 2dx - x^2$.

Case 4. $A(d) = 2d^2 - (d-x)^2 - (d-y)^2 = 2d(x+y) - (x^2+y^2)$.

Case 5. $A(d) = (d+y)x - x^2/2 + d^2/2 + dy - y^2/2 = d^2/2 + d(x+y) - (1/2)(x-y)^2$.

Case 6. $A(d) = 2d^2 - (d-y)^2 - (d+y-w)^2 = 2wd - 2y^2 + 2wy - w^2$.

Case 7. $A(d) = 2d^2 - (d-x)^2 - (d-y)^2 - (d+y-w)^2 = -d^2 + 2d(x+w) - 2y^2 + 2wy - x^2 - w^2$.

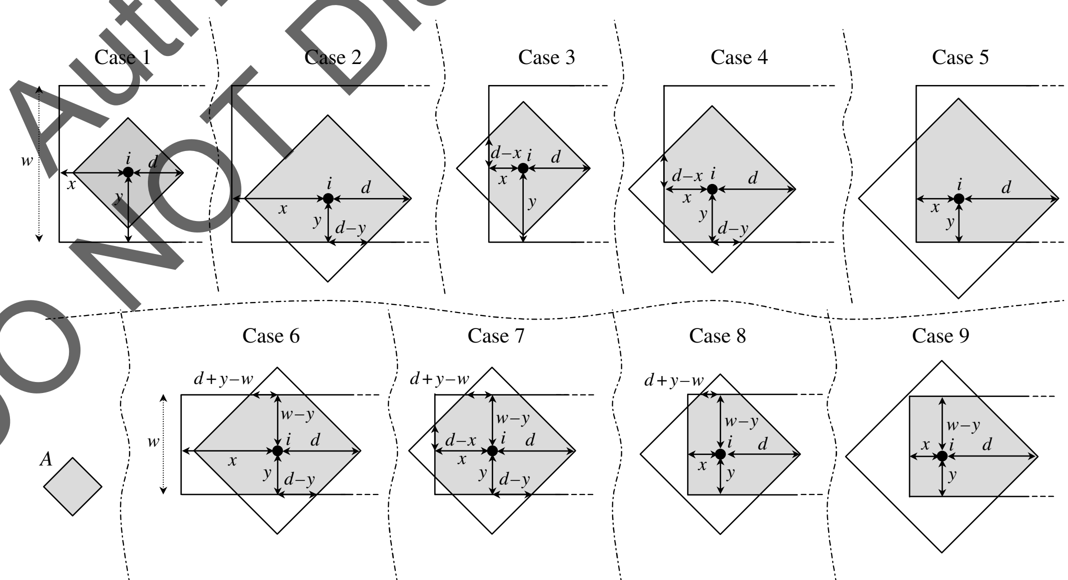

Figure 6 *A* **Depending on** x, y, **and** d

Authors Personal Copy
DO NOT Distribute or Reproduce

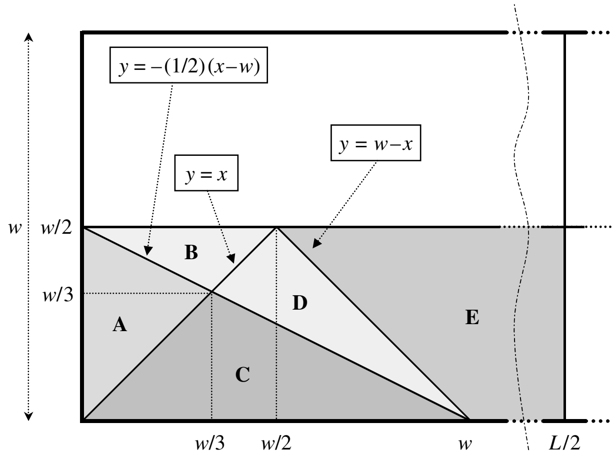

Figure 7 Zones with Different Sequence of Cases to Compute $A(d)$ with Increasing d

Case 8. $A(d) = (d+y)x - x^2/2 + d^2/2 + dy - y^2/2 - (d+y-w)^2 = -d^2/2 + d(x-y+2w) - x^2/2 + xy - 3y^2/2 + 2wy - w^2$.

Case 9. $A(d) = w(d+x) - (w-y)^2/2 - y^2/2 = wd + w(x+y) - y^2 - w^2/2$.

The expected value of D depending on x and y is given by

$$E[D(x,y)] = \int_0^\infty F(d)\,\mathrm{d}d = \int_0^\infty e^{-\rho A(d)}\,\mathrm{d}d. \tag{20}$$

The sequence of scenarios and formulas to be used to compute $A(d)$ in Equation (20) with increasing d is different depending on the zone in which $i(x,y)$ is located (see Figure 7 and Table 3).

Averaging over all values of x and y in the area considered we finally obtain

$$E[D] = \frac{4}{Lw}\int_0^{w/2}\int_0^{L/2} E[D(x,y)]\,\mathrm{d}x\,\mathrm{d}y. \tag{21}$$

Equation (21) does not have a closed-form expression, but we can examine two limiting scenarios depending on the value of the parameter $w\sqrt{\rho}$. This is an indication of the effect of the top and bottom edges of the strip on the calculation of $E[D]$.

If $w\sqrt{\rho} \to \infty$, we can approximate $E[D]$ by computing $A(d)$ only for Case 1. For the majority of the points, the probability of finding the closest point in an area defined by other cases is negligible, either because the edges are too far (large w) or because the density ρ is very high. Therefore,

$$E[D \mid w\sqrt{\rho} \to \infty] \approx \int_0^\infty e^{-2\rho d^2}\,\mathrm{d}d = \frac{1}{2}\sqrt{\frac{\pi}{2\rho}} \approx \frac{0.63}{\sqrt{\rho}}. \tag{22}$$

If $w\sqrt{\rho} \to 0$ and ignoring the effect of the left edge of the rectangle, we can approximate $E[D]$ by computing $A(d)$ only for Case 6. For the majority of the points, the probability of finding the closest point in an area defined by Case 1 and 2 is negligible, either because w is very small or the density is very low. Therefore, we obtain

$$E[D \mid w\sqrt{\rho} \to 0] \approx \frac{2}{w}\int_0^{w/2}\int_0^\infty e^{-\rho[2wd-2y^2+2wy-w^2]}\,\mathrm{d}d\,\mathrm{d}y = \frac{1}{2\rho w}. \tag{23}$$

This also corresponds to the expected distance of the closest point (in either direction) in a one-dimensional case with all the points uniformly distributed along a line with linear density ρw.

We performed numerical integrations on Equations (20) and (21) with $w = 0.5$ miles for three values of L (2, 6, and ∞ miles) and different values of ρ. The results are shown in Figure 8 along with the figures computed by simulations (10,000 replications for each ρ considered).

Int and *Sim* refer respectively to the data computed by numerical integration and simulation for each L. *Limit 1* and *Limit 2* refer to Equations (22) and (23), respectively. The *Int* data closely match the corresponding *Sim* data especially for higher ρ, confirming the negligible effect of the ignored right edge when performing the numerical integration. For lower ρ and lower L the discrepancies are slightly more noticeable also because the spatial Poisson

Table 3 Sequence of Cases to Compute $A(d)$ with Increasing d, for Each Zone

	Zone				
Case	A	B	C	D	E
1	$0 \le d \le x$	$0 \le d \le x$	$0 \le d \le y$	$0 \le d \le y$	$0 \le d \le y$
2			$y \le d \le x$	$y \le d \le x$	$y \le d \le w-y$
3	$x \le d \le y$	$x \le d \le y$			
4	$y \le d \le x+y$	$y \le d \le w-y$	$x \le d \le x+y$	$x \le d \le w-y$	
5	$x+y \le d \le w-y$		$x+y \le d \le w-y$		
6					$w-y \le d \le x$
7		$w-y \le d \le x+y$		$w-y \le d \le x+y$	$x \le d \le x+y$
8	$w-y \le d \le w-y+x$	$x+y \le d \le w-y+x$	$w-y \le d \le w-y+x$	$x+y \le d \le w-y+x$	$x+y \le d \le w-y+x$
9	$d \ge w-y+x$	$d \ge w-y+x$	$d \ge w-y+x$	$d \ge w-y+x$	$d \ge w-y+x$

Author's Personal Copy
DO NOT Distribute or Reproduce

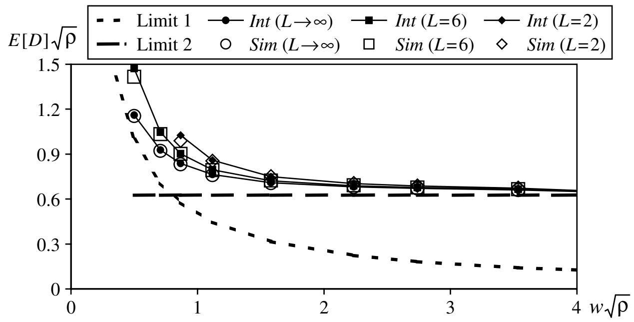

Figure 8 $E[D]$ **vs. Simulation and Asymptotic Limits**

distribution becomes less accurate when the total number of stops in the rectangle is too low. The chart shows that the curves are asymptotically bounded by the two limits for $w\sqrt{\rho} \to 0$ and $w\sqrt{\rho} \to \infty$ as expected. The left edge has the effect of increasing $E[D]$ with decreasing ρ and this becomes more relevant with decreasing L, in fact, the three curves diverge for $w\sqrt{\rho} \to 0$.

Assuming that the vehicle travels $E[D]$ miles from each stop (including the starting checkpoint) to its closest neighbor, the expected values of p and t in this case are given by

$$E[p] = (n+1)E[D] \quad \text{and} \tag{24}$$

$$E[t] = \frac{E[p]}{v} + ns = \rho w L\left[\frac{E[D]}{v} + s\right] + \frac{E[D]}{v}. \tag{25}$$

Finally, the second upper bound on V^* is formally given by $E[L/t]$, that is well approximated by $L/E[t]$ (with t far from 0 and $\mathrm{Var}[t]$ small) and, therefore, $V^{U''}$ is given by

$$V^{U''} \cong \frac{L}{E[t]} = \frac{v}{\rho w(E[D] + sv) + E[D]/L}. \tag{26}$$

As for V^L and V^U, $V^{U''}$ is inversely proportional to w, s, and ρ.

As done for V^L and V^U, we can verify by Table 4 the good estimates provided by Equation (26) on the true upper bound $E[L/t]$ computed by simulation for different values of ρ (10,000 replications for each ρ, with $w = 0.5$ miles, $L = 6$ miles). We also include a column with the values computed with Equation (26) utilizing the $E[D]$ values for $L = \infty$.

Table 4 $V^{U''}$ **Values: Analytical vs. Simulation**

	$V^{U''}$ (miles/hour)		
	Equation (26)		Simulation
ρ	$L=\infty$	$L=6$	$L=6$
1	33.38	27.14	29.12
5	19.54	19.07	18.97
10	12.46	12.35	12.30
50	3.49	3.48	3.48
100	1.90	1.90	1.90

Note that the simulation values are upper bounded by the values obtained with Equation (26) for $\rho > 1$. In addition, the values calculated by Equation (26) with $L = \infty$ are a tight upper bound of the ones with $L = 6$ miles, showing that they could be used conservatively to estimate $V^{U''}$ for any value of L. Moreover, when $\rho \to \infty$, by applying Equation (22) and ignoring the starting checkpoint, the asymptotic value for $V^{U''}$ is given by

$$\lim_{\rho\to\infty} V^{U''} = \frac{v}{\rho w s v + 0.63 w\sqrt{\rho}}. \tag{27}$$

8. Approximate Value for V^*

We know by Beardwood, Halton, and Hammersley (1959) and Jaillet (1988) that the length T of the optimal TSP tour for rectilinear metric visiting M points distributed randomly in a region of area A is approximated by the following formula:

$$T = 0.97\sqrt{AM}. \tag{28}$$

This formula provides better approximations with large values of M.

To make use of this result for our case, we assume that the MAST vehicle is driving along a long corridor that is shaped as a loop, having the starting and ending checkpoint coincide. With $L \gg w$, we can approximate the ring-shaped service area as $A = wL$ and estimate the optimal length of the tour by Equation (28) for different values of $M = \rho A = \rho w L$. Because the total time t_a spent to complete a loop is given by

$$t_a = \frac{T}{v} + Ms = Lw\sqrt{\rho}\left(\frac{0.97}{v} + \sqrt{\rho}s\right), \tag{29}$$

the resulting approximation of the optimal longitudinal velocity V^A is given by

$$V^A = \frac{L}{t_a} = \frac{v}{\rho w s v + 0.97 w\sqrt{\rho}}, \tag{30}$$

which has the same form as the asymptotic value of $V^{U''}$ for $\rho \to \infty$, given by Equation (27), with 0.97 replacing 0.63. As for V^L, V^U, and $V^{U''}$, V^A is inversely proportional to w, s, and ρ. However, V^A goes to infinity when ρ goes to zero, confirming that Equation (30) does not provide good estimates for low ρ. We need to emphasize that V^A is neither an upper nor a lower bound of V^*, and it does not consider the customer precedence constraints.

Authors Personal Copy
DO NOT Distribute or Reproduce

9. Performance Evaluation and Design Issues

We are now able to plot the lower bound V^L, the upper bounds V^U and $V^{U''}$, and the approximate value V^A, respectively, using Equations (7), (17), (26), and (30). In addition, we computed V^I representing the longitudinal velocity while implementing an insertion heuristic algorithm minimizing the distance traveled to schedule the uniformly distributed demand. Insertion algorithms generally provide good feasible solutions and are widely used for scheduling DRT systems, but they do not guarantee optimality. Thus, the resulting values represent a lower bound for V^* as well. However, they cannot be quickly computed for any scenario like V^L because they do not have closed-form expressions and are obtained by simulation (1,000 replications averaged for each ρ considered).

We analyze two different cases, with $L = 6$ miles and $w = 0.5$ miles (see Figure 9) consistent with the existing MAST system (Line 646 in Los Angeles County), and $L = 6$ miles and $w = 1$ mile (see Figure 10). As mentioned in §3, we also assume $v = 30$ miles/hour and $s = 30$ seconds.

We note that in both charts V^L and V^U converge for lower values of ρ because they both provide better estimates for lower ρ. $V^{U''}$ is a tighter bound than V^U for higher ρ and this is more evident for the case with $w = 1$ mile. The gap between V^L and $V^U/V^{U''}$ does not diverge significantly with increasing ρ maintaining a reasonably narrow range. The approximate value V^A falls in the middle of this range, except for smaller ρ, because V^A is no longer a good estimate for low-demand density. The insertion heuristic curve V^I lies a little above V^L; the gap between them slightly increases with ρ, showing that the improvement provided by the insertion heuristic algorithm over the no-backtracking policy is more evident for denser demand. This gap is smaller for $w = 0.5$ miles,

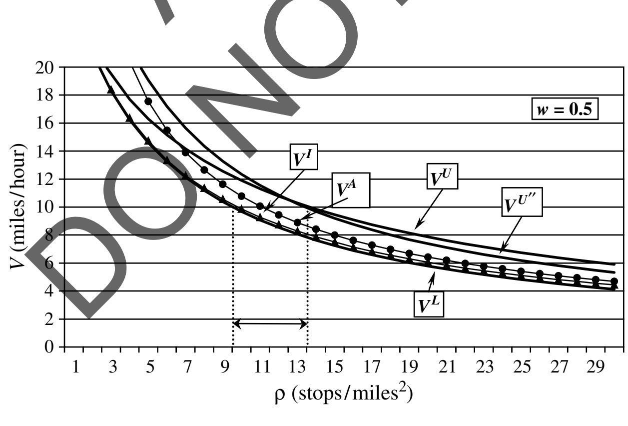

Figure 9 **Longitudinal Velocity** (V) **vs. Demand Density** (ρ); $w = 0.5$ **Miles**

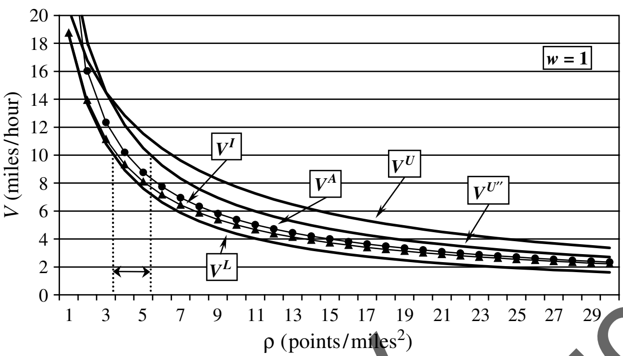

Figure 10 **Longitudinal Velocity** (V) **vs. Demand Density** (ρ); $w = 1$ **Mile**

because the narrower corridor guarantees better solutions from the no-backtracking policy (in accordance with Proposition 1).

Even though MAST services are designed to provide a comfortable door-to-door service, customers would probably perceive the service as being too slow if the velocity along the primary direction would fall below a threshold value. According to a random check of the timetables of various fixed-route bus lines in Los Angeles County, regular fixed-route buses generally achieve an overall average velocity along their routes of about 15 miles per hour, depending on the number of stops placed in the route and the number of customers to be served (they can go as fast as 20 miles/hour for interurban fast lines and they can go as slow as 10 miles/hour for downtown services). The demand will generally vary depending on different factors, but typically the faster the service the higher the demand. However, we assume that customers would be willing to sacrifice some of this velocity for the convenience of being picked up and dropped off at their desired locations. We observe that ρ represents the density of the stops of customers that are either picked up or dropped off (or both) in a random location. MAST systems also serve the regular customers that rely on already-scheduled checkpoints for both their service points, not requiring any deviations from the main route. Thus, the latter type of customers clearly would not welcome a slower service. Therefore, the allowed reduction on the longitudinal velocity should be tailored to the customers' type distribution: the more customers are regular, the faster the service should be.

The existing MAST Line 646 serves a very low at night demand of about $\rho = 1$–2 customers/miles²; the width of the service area is about $w = 0.5$ miles that allows the system to properly serve all the customers, maintaining a relatively high longitudinal velocity of 25 miles/hour. Heavier demands would require either a lower longitudinal velocity while maintaining the

Author's Personal Copy
DO NOT Distribute or Reproduce

same service area, a narrower width of the strip keeping the same longitudinal velocity, or more vehicles, thereby reducing the cycle length.

As an example, we assume the minimum acceptable V of a MAST system to be 10 miles/hour, 33% less than that of average fixed-route buses; we suppose that below this level the demand would radically drop because it is too inconvenient. From the charts we note that the demand density that can be served corresponding to the value of $V = 10$ miles/hour is in the range of $\rho = 9.5$–13.5 customers/mile^2 (when $w = 0.5$ miles) and $\rho = 3.5$–5.5 customers/mile^2 (when $w = 1$ mile), according to the values provided by the bounds. Recall that ρ represents the density of the stops served only by the left-right vehicle and the total density served by both vehicles is 2ρ. Therefore, the system would be able to serve at least $2 \times 9.5 \times 0.5 \cong 10$ stops every mile of the corridor (when $w = 0.5$ miles) and $2 \times 3.5 \times 1 = 7$ stops every mile of the corridor (when $w = 1$ mile).

In Figures 11 and 12 we also show the relationships between the demand and the total capacity ($K = \rho w V$ stops/hour) of the system, considering both vehicles. K^L, K^U, $K^{U''}$, K^A, and K^I plot the values of the capacity for each ρ and correspond to the velocity curves in the V/ρ charts with the same superscript. The ranges of density and capacity corresponding to $V = 10$ miles/hour are highlighted.

The MAST system would be able to serve between 90 and 130 stops per hour for the case with $w = 0.5$ miles, maintaining a longitudinal velocity $V = 10$ miles/hour, and between 70 and 120 stops per hour for the case with $w = 1$ mile. This result suggests that doubling the width of the service area does not substantially affect the performance of the system in terms of its capacity. The capacity K, like the velocity V, is inversely proportional to the values of s and v.

When designing a MAST system, planners can make use of the information provided in the above charts to schedule the time difference between checkpoints, thereby setting the velocity of the service and establishing the maximum slack time allowed for

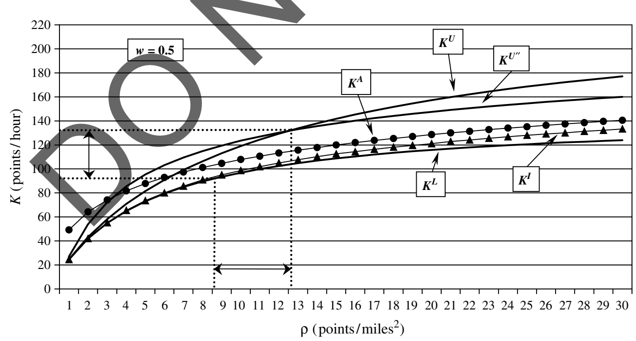

Figure 11 Capacity (K) vs. Demand Density (ρ); $w = 0.5$ Miles

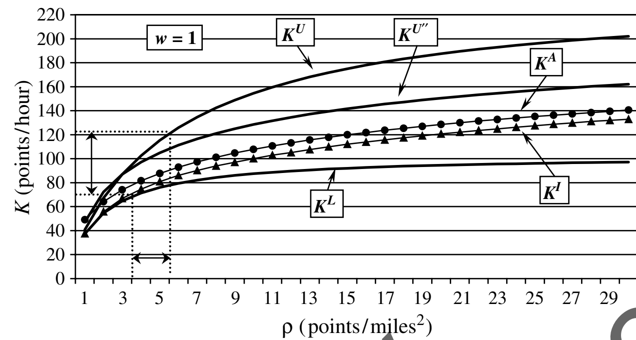

Figure 12 Capacity (K) vs. Demand Density (ρ); $w = 1$ Mile

deviations. For example, with the assumed minimum acceptable longitudinal velocity of $V = 10$ miles/hour and $L = 6$ miles, the time interval between the checkpoints considered would be $\Delta t = L/V = 36$ minutes, with a slack time of about 23 minutes, enough to serve about $10 \times L = 60$ noncheckpoint stops (30 per vehicle) when $w = 0.5$ miles. In addition, knowing the actual total demand rate in the service area, it would be possible to choose the headway and assign the number of vehicles to the line to satisfy it properly.

10. Conclusions

We evaluated upper and lower bounds on the maximum longitudinal velocity of a MAST vehicle using continuous approximations. We also provided values for the longitudinal velocity from approximation formulas and simulation using an insertion heuristic algorithm. The gap between the bounds remains relatively small with varying demand and provides us with a useful tool to evaluate the performance of MAST systems. Results show that the system is able to properly serve a reasonable demand while maintaining a relatively high velocity. While the longitudinal velocity of the vehicle is considerably affected by a widening of the service area, the capacity of the system (in terms of customers served per hour) is only slightly influenced. The relationships between velocity and capacity versus demand density can be beneficially used in the design process to set the slack time between checkpoints and other parameters of the MAST system.

Future research on MAST systems could focus on studying the system under different demand distributions and designing efficient networks of this type of service to cover wider service areas. The combinatorial nature of the problem would also require the development and analyses of efficient algorithms to schedule the vehicles interconnected in these networks.

Acknowledgments

The research reported in this paper was partially supported by the National Science Foundation under Grant NSF/USDOT-0231665.

DO NOT Distribute or Reproduce
Author's Personal Copy

Appendix

As an example related to §6, we want to derive the expected value of n_G for when $n=2$ and $n=3$ stops. The longitudinal coordinate x_i of each of the stops is uniformly distributed in $[0, L]$.

$n=2$

The probability of having only one point in G is the probability of having both points included in a longitudinal interval of at most w, thus given by

$$P\{n_G=1 \mid n=2\} = (n!)P\{x_1 \le x_2 \le x_1+w\}$$
$$= \frac{2}{L^2}\left(\int_0^{L-w}\int_{x_1}^{x_1+w} \mathrm{d}x_2\,\mathrm{d}x_1 + \int_{L-w}^{L}\int_{x_1}^{L} \mathrm{d}x_2\,\mathrm{d}x_1\right)$$
$$= 2\frac{w}{L} - \frac{w^2}{L^2}, \tag{31}$$

while the probability of having two points in G is the complement and thus given by

$$P\{n_G=2 \mid n=2\} = 1 - P\{n_G=1 \mid n=2\}$$
$$= 1 - 2\frac{w}{L} + \frac{w^2}{L^2}. \tag{32}$$

Thus, the expected value of n_G with $n=2$ is given by

$$E[n_G \mid n=2] = \sum_{i=1}^{2} i \times P\{n_G=i \mid n=2\} = 2 - 2\frac{w}{L} + \frac{w^2}{L^2}. \tag{33}$$

$n=3$

The probability of having only one point in G is the probability of having all three points included in a longitudinal interval of at most w, thus given by

$$P\{n_G=1 \mid n=3\}$$
$$=(n!)P\{x_1 \le x_2 \le x_3 \le x_1+w\}$$
$$= \frac{6}{L^3}\left(\int_0^{L-w}\int_{x_1}^{x_1+w}\int_{x_2}^{x_1+w} \mathrm{d}x_3\,\mathrm{d}x_2\,\mathrm{d}x_1 + \int_{L-w}^{L}\int_{x_1}^{L}\int_{x_2}^{L} \mathrm{d}x_3\,\mathrm{d}x_2\,\mathrm{d}x_1\right)$$
$$= 3\frac{w^2}{L^2} - 2\frac{w^3}{L^3}. \tag{34}$$

The probability of having all three points in G is the probability of having them longitudinally distant from each other at least w and therefore is given by

$$P\{n_G=3 \mid n=3\} = (n!)P\{x_1+2w \le x_2+w \le x_3\}$$
$$= \frac{6}{L^3}\int_0^{L-2w}\int_{x_1+w}^{L-w}\int_{x_2+w}^{L} \mathrm{d}x_3\,\mathrm{d}x_2\,\mathrm{d}x_1$$
$$= 1 - 6\frac{w}{L} + 12\frac{w^2}{L^2} - 8\frac{w^3}{L^3}. \tag{35}$$

Finally, the probability of having two points in G is the complement and therefore given by

$$P\{n_G=2 \mid n=3\} = 1 - P\{n_G=1 \mid n=3\} - P\{n_G=3 \mid n=3\}$$
$$= 6\frac{w}{L} - 15\frac{w^2}{L^2} + 10\frac{w^3}{L^3}. \tag{36}$$

Thus, the expected value of n_G with $n=3$ is given by

$$E[n_G \mid n=3] = \sum_{i=1}^{3} i \times P\{n_G=i \mid n=3\}$$
$$= 3 - 6\frac{w}{L} + 9\frac{w^2}{L^2} - 6\frac{w^3}{L^3}. \tag{37}$$

References

Aldaihani, M. M., M. M. Dessouky. 2003. Hybrid scheduling methods for paratransit operations. *Comput. Indust. Engrg.* **45** 75–96.

Aldaihani, M. M., L. Quadrifoglio, M. M. Dessouky, R. W. Hall. 2004. Network design for a grid hybrid transit service. *Transportation Res. Part A* **38** 511–530.

Beardwood, J., J. H. Halton, J. M. Hammersley. 1959. The shortest path through many points. *Proc. Cambridge Philos. Soc.* **55** 299–327.

Bouwkamp, C. J. 1977. On the average distance between points in two coplanar non-overlapping circular disks. *J. Appl. Sci. Engrg.* **A2** 183–186.

Ceder, A., N. H. M. Wilson. 1986. Bus network design. *Transportation Res. Part B* **20** 331–344.

Chang, S. K., P. M. Schonfeld. 1991a. Multiple period optimization of bus transit systems. *Transportation Res. Part B* **25** 453–478.

Chang, S. K., P. M. Schonfeld. 1991b. Optimization models for comparing conventional and subscription bus feeder services. *Transportation Sci.* **25** 281–298.

Chien, S., P. M. Schonfeld. 1997. Optimizing of grid transit system in heterogeneous urban environment. *J. Transportation Engrg.* **123** 28–35.

Christofides, N., S. Eilon. 1969. Expected distances in distribution problems. *Oper. Res. Quart.* **20** 437–443.

Cortés, C. E., R. Jayakrishnan. 2002. Design and operational concepts of a high coverage point-to-point transit system. *Transportation Res. Record* **1783** 178–187.

Crainic, T. G., F. Malucelli, M. Nonato. 2001. Flexible many-to-few + few-to-many = an almost personalized transit system. *TRISTAN IV*, São Miguel, Azores Islands, Portugal, 435–440.

Daganzo, C. F. 1978. An approximate analytic model of many-to-many demand responsive transportation systems. *Transportation Res.* **12** 325–333.

Daganzo, C. F. 1980. Network representation, continuum approximations and a solution to the spatial aggregation problem of traffic assignment. *Transportation Res. Part B* **14** 229–239.

Daganzo, C. F. 1984a. The length of tours in zones of different shapes. *Transportation Res. Part B* **18** 135–145.

Daganzo, C. F. 1984b. The distance traveled to visit N points with a maximum of C stops per vehicle: An analytic model and an application. *Transportation Sci.* **18** 331–350.

Daganzo, C. F. 1984c. Checkpoint dial-a-ride systems. *Transportation Res. Part B* **18** 315–327.

Daganzo, C. F. 1991. *Logistic Systems Analysis. Lecture Notes in Economics and Mathematical Systems*, No. 361. Springer-Verlag, Heidelberg, Germany.

Dessouky, M. M., F. Ordóñez, L. Quadrifoglio. 2005. Productivity and cost-effectiveness of demand responsive transit systems. PATH/Caltrans Technical Report, Berkeley, CA.

Diana, M., M. M. Dessouky, N. Xia. 2006. A model for the fleet sizing of demand responsive transit services with time windows. *Transportation Res. Part B* Forthcoming.

Faithorne, D. 1965. Distances between pairs of points in towns of simple geometrical shapes. *Proc. 2nd Internat. Sympos. Theory Traffic Flow*, OECD, Paris, France, 391–406.

Ghosh, B. 1951. Random distances within a rectangle and between two rectangles. *Bull. Calcutta Math. Soc.* **43** 17–24.

Hall, R. W. 1986. Discrete models/continuous models. *Omega Internat. J. Management Sci.* **14** 213–220.

Horn, M. E. T. 2002a. Multi modal and demand responsive passenger transport systems: A modeling framework with embedded control systems. *Transportation Res. Part A* **36** 167–188.

Horn, M. E. T. 2002b. Fleet scheduling and dispatching for demand responsive passenger services. *Transportation Res. Part C* **10** 35–63.

Author's Personal Copy
DO NOT Distribute or Reproduce

Jacobson, J. 1980. Analytical models for comparison of alternative service options for the transportation handicapped. *Transportation Res. Part A* **14** 113–118.

Jaillet, P. 1988. A priori solution of a traveling salesman problem in which a random subset of the customers are visited. *Oper. Res.* **36** 929–936.

Koshizuka, T., O. Kurita. 1991. Approximate formulas of average distances associated with regions and their applications to location problems. *Math. Programming* **52** 99–123.

Kuah, G. K., J. Perl. 1988. Optimization of feeder bus routes and bus-stop spacing. *J. Transportation Engrg.* **114** 331–354.

Langevin, A., P. Mbaraga, J. F. Campbell. 1996. Continuous approximation models in freight distribution: An overview. *Transportation Res. Part B* **30** 163–188.

LeBlanc, L. J. 1988. Transit system network design. *Transportation Res. Part B* **22** 383–390.

Lesley, L. J. S. 1976a. Optimum bus-stop spacing: Part 1. *Traffic Engrg. Control* **17** 399–401.

Lesley, L. J. S. 1976b. Optimum bus-stop spacing: Part 2. *Traffic Engrg. Control* **17** 472–473.

Malucelli, F., M. Nonato, S. Pallottino. 1999. Demand adaptive systems: Some proposals on flexible transit. T. Ciriania, E. Johnson, R. Tadei, eds. *Operations Research in Industry*. 157–182.

Mandl, C. E. 1980. Evaluation and optimization of urban public transport networks. *Eur. J. Oper. Res.* **6** 31–56.

Newell, G. F. 1979. Some issues relating to the optimal design of bus routes. *Transportation Sci.* **13** 20–35.

Quadrifoglio, L., M. M. Dessouky, K. Palmer. 2006. An insertion heuristic for scheduling mobility allowance shuttle transit (MAST) services. *J. Scheduling*. Forthcoming.

Rhee, W. T. 1993. On the stochastic traveling salesperson problem for distributions with unbounded support. *Math. Oper. Res.* **18** 252–259.

Ruben, H. 1978. On the distance between points in polygons. R. Miles, J. Serra, eds. *Lecture Notes in Biomathematics*, No. 23. Springer-Verlag, Berlin, Germany.

Schweitzer, P. A. 1968. Moments of distances of uniformly distributed points. *Amer. Math. Monthly* **75** 802–804.

Stadje, W. 1995. Two asymptotic inequalities for the stochastic traveling salesman problem. *Sankhya: Indian J. Statist.* **57A1** 33–40.

Stein, D. M. 1978. Scheduling dial-a-ride transportation problems. *Transportation Sci.* **12** 232–249.

Stone, R. E. 1991. Some average distance results. *Transportation Sci.* **25** 83–91.

Szplett, D. B. 1984. Approximate procedures for planning public transit systems: A review and some examples. *J. Advanced Transportation* **18** 245–257.

Vaughan, R. J. 1984. Approximate formula for average distances associated with zones. *Transportation Sci.* **18** 231–244.

Verblunsky, S. 1951. On the shortest path through a number of points. *Proc. Amer. Math. Soc.* **6** 904–913.

Wirasinghe, S. C., N. S. A. Ghoneim. 1981. Spacing of bus-stops for many-to-many travel demand. *Transportation Sci.* **15** 210–221.

Zhao, J., M. M. Dessouky. 2004. Optimal service capacity for a single-bus mobility allowance shuttle transit (MAST) system. Working paper.

Author's Personal Copy
DO NOT Distribute or Reproduce